Thermoelectric power factor in nano- to microscale porous composites

Roland H. Tarkhanyan[a)]
Institute of Nanoscience and Nanotechnology, National Center for Scientific Research "Demokritos", Athens 15310, Greece; and Institute of Radiophysics & Electronics, National Academy of Sciences of Armenia, Ashtarak 0203, Armenia

Dimitris G. Niarchos
Institute of Nanoscience and Nanotechnology, National Center for Scientific Research "Demokritos", Athens 15310, Greece

(Received 23 November 2014; accepted 5 May 2015)

The peculiarities of the Seebeck coefficient and power factor are studied in porous thermoelectric materials with spherical hollow pores of varying diameter from nanometer to micrometer length scales. The pores are assumed to be randomly dispersed throughout the matrix material. The influence of trap centers situated at pore interfaces on the power factor is investigated. Using the model based on gamma distribution of the pore sizes, the analytical expression is obtained for the power factor at the arbitrary level of the Fermi energy. Limiting cases of nondegenerate and degenerately doped porous semiconductors are examined as well. The results are compared with calculations for a multilayer composite in which each layer contains pores of a single length-scale. It is shown that the presence of hollow pores with multiscale hierarchical disorder leads to more considerable enhancement in the thermopower over its value in the bulk. Necessary conditions for the enhancement of the power factor are found.

I. INTRODUCTION

In recent years, granular nanocomposites and porous materials have attracted extensive interest because of their potential as candidates for increasing the dimensionless thermoelectric figure-of-merit $ZT = \sigma S^2 T/\kappa$, where σ is the electrical conductivity, S is the Seebeck coefficient, κ is the thermal conductivity, and T is the average absolute temperature.[1–6] For most of the commercially available thermoelectric materials, ZT is well below one. This fact limits the efficiency of energy conversion between electricity and heat, and the application of thermoelectric devices for power generation and refrigeration. In 2002, Harman et al. reported $ZT = 1.6$ at $T = 300$ K for PbSeTe/PbTe nanodot superlattices.[7] Recently, a dramatic enhancement in ZT has been achieved in bulk thermoelectric nanostructures with all-scale hierarchical architecturing for lead chalcogenides PbTe, PbSe, and PbS.[8,9,10] A recorded high ZT value of ~2.2 at 915 K has been demonstrated by the introduction of 1–17 nm SrTe nanoscale precipitations and 0.1–1 μm micrograins in the Na-doped PbTe matrix.[9] The increase in ZT value has come either from the reduction in lattice thermal conductivity or improvement in thermoelectric power factor $P = \sigma S^2$, or both of them. Note that there are many theoretical and experimental studies on the enhancement of the Seebeck coefficient and power factor (see, e.g., Refs. 11,12,13,14 and citations therein). In Ref. 14, it has been reported a large power factor in p-type nanocrystalline Si: ~5 times higher than in bulk Si. Assuming inhomogeneous impurity distribution in grains, a theoretical model has been developed to show the increase in electrical conductivity in the grains and simultaneous increase in the Seebeck coefficient in grain boundaries.

Despite such a rapid progress in technology of high-performance thermoelectric materials, very few theoretical works have, yet, been done to analyze thermal transport properties in semiconductors with pores or inclusions of varying size scales. In our recent publications,[15,16] a considerable reduction in lattice thermal conductivity of a nanocomposite with pores from nano to microscale size has been predicted. In Ref. 17, we have shown that the porosity always leads to an increase in the absolute value of the Seebeck coefficient due to the enhancement of the entropy per charge carrier. This enhancement is caused by the energy-filtering effect at pore boundaries and reduction of the carrier's density compared to that in bulk material with zero porosity. The pores were assumed to be periodically distributed and identical in each layer.

Contributing Editor: Terry M. Tritt
[a)]Address all correspondence to this author.
e-mail: rolandtarkhanyan@yahoo.com;
tarkhanyan@ims.demokritos.gr
DOI: 10.1557/jmr.2015.151

 © Materials Research Society 2015

https://doi.org/10.1557/jmr.2015.151 Published online by Cambridge University Press

The purpose of this work is an investigation of opportunities for the enhancement in the thermopower and power factor of porous structures with all-scale hierarchical disorder in the size of the pores, which are assumed randomly dispersed throughout the matrix material. We will examine how the presence of randomly distributed pores can vary electrical conductivity and the Seebeck coefficient of porous materials, aiding the design of better thermoelectric materials with higher figure-of-merit *ZT*. Since a porous medium has a high surface area per unit volume, it is very important to take into account the possibility of trapping for free charge carriers in deep energetic states localized at pore/medium interfaces. For definiteness and simplicity, we will restrict ourselves to the consideration of n-type isotropic thermoelectric host material with single parabolic conduction band. As in Ref. 17, we will neglect possible changes in the carrier effective mass due to the band bend at pore–medium interfaces and assume that there are no charge carriers inside the pores, which are hollow or filled by insulating nano- or microinclusions. In other words, the pore boundaries are considered as energy barriers with high-scattering potential so as the low energy electrons scatter strongly (i.e., the transmission probability is negligible), while the high-energy ones are practically unaffected. We will show that in the presence of pores of different size scales in the same host material, it is possible to achieve a considerable improvement in the Seebeck coefficient (S) over its value in the bulk material. The enhancement in S in this case is stronger than in a multilayer composite, different layers of which contain only pores of a single length-scale. The enhancement in power factor (P) is only possible if the relative growth in S exceeds a definite critical value, which depends on the position of the Fermi energy. We will determine these critical values for both nondegenerate and degenerately doped porous semiconductors.

The paper is organized as follows: in the next section, the details of modeling for a porous material with randomly distributed spherical nonoverlapping hollow pores of different size scales are given, and the porosity of such a material is determined on the base of the gamma distribution for pore sizes. In Sec. III, the presence of trap centers localized at interfaces of the pores is taken into account, and their influence on the chemical potential is examined in both nondegenerate and degenerately doped porous semiconductors. In Sec. IV, we derive an analytical expression for the power factor in the presence of different groups of pores with various length-scales in host material, at the arbitrary level of the Fermi energy. In Sec. V, we examine the peculiarities of the Seebeck coefficient, electrical conductivity, and power factor in limiting cases of nondegenerate and degenerately doped materials and show that the presence of hollow pores with all-scale hierarchical disorder leads to a considerable enhancement in the thermopower. The necessary conditions for the enhancement of the power factor are found. In Sec. VI, we consider the effective thermopower and electrical conductivity of a multilayer composite consisting of alternating layers of various porosities with pores of the same size scale in each layer and show that when the pores of different size scales are situated in the same host material, it is possible to achieve stronger enhancement in both S and P than in the multilayer composite. Finally, in Sec. VII, we make concluded remarks.

II. PORE SIZE DISTRIBUTION AND NET POROSITY

Consider a porous medium in the presence of different groups of nonoverlapping spherical hollow pores with various size scales, e.g., nanoscale pores with randomly distributed pore diameters $d_1 < 100$ nm around average diameter $\overline{d_1}$, microscale ones with diameters $d_3 \geq 1$ μm around average diameter $\overline{d_3}$, and pores with intermediate size diameters d_2 around average diameter $\overline{d_2}$ (Fig. 1). As in Refs. 15 and 16, we assume that the pore size distribution in each group is described by probability density function

$$f(\rho_i) = \frac{N(\rho_i)}{N_i} = \frac{\rho_i^{\alpha_i - 1} \exp(-\rho_i/\beta_i)}{\beta_i^{\alpha_i}\Gamma(\alpha_i)}, \quad i = 1, 2, 3 \quad , \tag{1}$$

where $\rho_i = d_i/\overline{d_i}$ are the nondimensional diameters, $N(\rho_i)d\rho_i$ is the number of pores with given size scale in the interval, $\rho_i, \rho_i + d\rho_i, N_i$ is the total number of pores in the group, $\alpha_i > 1$ and β_i are the "shape" and "scale" parameters of the gamma distribution, respectively,[18] and $\Gamma(\alpha_i)$ is the gamma function (the Euler integral of the second kind). The mean (first moment) and variance of the distribution are given by $\alpha_i\beta_i = 1$ and $\alpha_i\beta_i^2 = \alpha_i^{-1}$, respectively, using which for the second and third moments of the distribution, one can obtain[15,16]

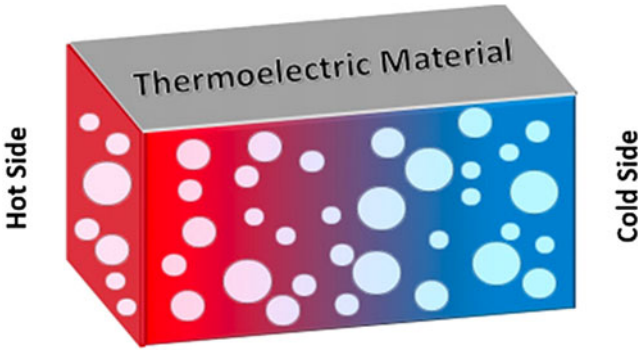


FIG. 1. Schematic illustration of the medium with randomly distributed nano, intermediate, and microscale pores.

https://doi.org/10.1557/jmr.2015.151 Published online by Cambridge University Press

$$\overline{\rho_i^2} = 1 + \alpha_i^{-1} \quad , \tag{2}$$

$$\overline{\rho_i^3} = \frac{\beta_i^3 \Gamma(\alpha_i + 3)}{\Gamma(\alpha_i)} = \frac{(\alpha_i + 1)(\alpha_i + 2)}{\alpha_i^2} \quad . \tag{3}$$

Note that if the standard deviation $\alpha_i^{-1/2}\overline{\rho_i}$ is much less than the mean, i.e., when $\alpha_i^{1/2} \gg 1$, the distribution function $f(\rho_i) \sim \delta(\rho_i - \overline{\rho_i})$. The porosity φ_i of each group is given by

$$\varphi_i = V_i/V = \pi c_i \overline{d_i}^3 \overline{\rho_i^3} \Big/ 6 \quad , \tag{4}$$

where V is the total volume of the sample.

$$V_i = \pi \overline{d_i}^3 N_i \overline{\rho_i^3} \Big/ 6 \quad , \tag{5}$$

is the net volume of the pores with given size scale, and $c_i = N_i/V$ is the number density (concentration) of the pores. It is evident that the net porosity of the material is given by

$$\varphi = \sum_i \varphi_i \quad . \tag{6}$$

III. EFFECTIVE POROSITY AND FERMI ENERGY IN THE PRESENCE OF INTERFACE TRAP CENTERS

In porous materials under consideration, free charge carriers are absent not only inside the pores but also in a small spherical region around the pores due to the presence of deep surface states, which act as electron traps. These trap centers are situated at pore/medium interfaces and are characterized by localized energy E_{tr} near or above the middle of the band gap. Total number of traps per pore is then $\pi d_i^2 N_s$, where N_s is the areal density of trap centers. Consequently, the volume density of traps localized at interfaces of the pores with given size scale is equal to

$$N_{tr,i} = \pi d_i^2 N_s c_i = 6\varphi_i N_s \rho_i^2 \Big/ \overline{d_i \rho_i^3} \quad , \tag{7}$$

where c_i is eliminated with the use of Eq. (4). Usually $N_{tr,i} \ll N_D$, where N_D is the net density of shallow donors with energy of ionization ε_D. In the temperature range $\varepsilon_D < k_B T < \varepsilon_G/2$, where ε_G is the width of the band gap, all the donors are assumed to be ionized and then the density of electrons in bulk material $n_0 \cong N_D$. In porous material, as electrons are trapped, spherical regions depleted of free electrons are forming around the pores. Assuming that all trap states are filled by frozen-in electrons and there is no thermal emission from these states, the condition of electrical neutrality can be written as

$$\frac{4}{3}\pi \left[R_i^3 - \left(\frac{d_i}{2} \right)^3 \right] N_D q = \pi d_i^2 N_s q \quad , \tag{8}$$

using which for the radius of the depleted region, one can obtain

$$R_i = \frac{d_i}{2}\left(1 + \frac{6N_s}{d_i N_D} \right)^{1/3} \quad . \tag{9}$$

Thus, the volume per pore with no mobile electron is equal to $V_{p,i}(1 + 6N_s/N_D d_i)$, where $V_{p,i} = \pi d_i^3/6$ is a pore volume. Introducing now "effective porosity" with respect to mobile electrons for each group of the pores

$$\phi_i = \varphi_i \left[1 + \frac{6N_s \overline{\rho_i^2}}{N_D \overline{d_i} \overline{\rho_i^3}} \right] \quad , \tag{10}$$

for the net effective porosity and the effective density of free electrons in porous material we obtain, respectively,

$$\phi \equiv \sum_i \phi_i = \varphi + \varphi_{tr} \quad , \tag{11a}$$

and

$$n = n_0(1 - \phi) \quad , \tag{11b}$$

where

$$\varphi_{tr} = \frac{6N_s}{N_D} g, \quad g \equiv \sum_{i=1}^{3} \frac{\alpha_i \varphi_i}{(\alpha_i + 2)\overline{d_i}} \quad . \tag{12}$$

Thus, the presence of pores and traps leads to a reduction of free charge carriers' density with respect to that in bulk material with zero porosity and consequently to the shifting of the Fermi energy and modification of all transport coefficients. Consider, for example, n-type isotropic material with a single parabolic conduction band. The density of electrons at the arbitrary level of the Fermi energy is given by

$$n = \frac{(2m^* k_B T)^{3/2}}{2\pi^2 \hbar^3} F_{1/2}(\zeta^*) \quad , \tag{13}$$

where m^* is the effective mass, k_B is the Boltzmann constant, T is the absolute temperature, h is the Planck constant, ζ is the chemical potential relative to the conduction band edge, $\zeta^* \equiv \zeta/k_B T$ is the reduced chemical potential, and

https://doi.org/10.1557/jmr.2015.151 Published online by Cambridge University Press

$$F_n(\zeta^*) = \int_0^\infty \frac{x^n \mathrm{d}x}{\exp(x-\zeta^*)+1} \quad , \tag{14}$$

is the Fermi integral. Using Eq. (11b) in the case of nondegenerate semiconductors, where $\exp(-\zeta^*) \gg 1$, for the reduced chemical potential, we obtain

$$\zeta^* = \zeta_0^* + \ln(1-\phi) \quad , \tag{15a}$$

where

$$\zeta_0^* = -\ln(N_c/n_0) \quad , \tag{15b}$$

is the reduced chemical potential in bulk material with zero porosity, and

$$N_c = 2(2\pi m^* k_B T)^{3/2} \Big/ h^3 \quad , \tag{16}$$

is the effective density of states in the conduction band. Since ζ_0 is negative, from Eq. (15a), one can conclude that the presence of porosity leads to the enhancement in the absolute value of the Fermi level. Unlike this, in the case of degenerately doped materials, where $\exp(\zeta^*) \gg 1$, the Fermi energy decreases:

$$\zeta = \zeta_0(1-\phi)^{2/3} \quad , \tag{17}$$

Here

$$\zeta_0 = \varepsilon_F^0 \left[1 - \frac{\pi^2}{12}\left(\frac{k_B T}{\varepsilon_F^0}\right)^2\right] \quad , \tag{18a}$$

where

$$\varepsilon_F^0 = \frac{\hbar^2}{2m^*}\left(3\pi^2 n_0\right)^{2/3} \quad , \tag{18b}$$

is the Fermi energy at $T = 0$ K.

IV. POWER FACTOR IN THE PRESENCE OF DIFFERENT GROUPS OF PORES WITH VARIOUS SIZE SCALES

Consider now a composite with all-scale hierarchical disorder in pore sizes, e.g., a material consisting of different phases: host porous medium with volume fraction $1 - \varphi$ and different groups of nanoscale and microscale insulating particles (or hollow pores) with volume fractions φ_i. We will use classical expressions for the Seebeck coefficient and electrical conductivity based on the solution of the Boltzmann transport equation under relaxation time approximation. They can be written in the form

$$S = \frac{1}{qT}\left[\frac{G_{5/2}(\zeta^*)}{G_{3/2}(\zeta^*)} - \zeta\right] \quad , \tag{19}$$

$$\sigma = \frac{2q^2(2m^*)^{1/2}}{3\pi^2\hbar^3} G_{3/2}(\zeta^*) \quad , \tag{20}$$

using which for the power factor, one can obtain

$$P = \frac{2(2m^*)^{1/2}}{3\pi^2\hbar^3 T^2} \frac{\left(G_{5/2} - \zeta G_{3/2}\right)^2}{G_{3/2}} \quad , \tag{21}$$

where

$$G_n \equiv G_n(\zeta^*) = \int_0^\infty \varepsilon^n (-\partial f_0/\partial\varepsilon)\tau(\varepsilon)\mathrm{d}\varepsilon \quad . \tag{22}$$

$f_0(\varepsilon, T) = (\exp[(\varepsilon-\zeta)/k_B T] + 1)^{-1}$ is the Fermi distribution function, and $\tau(\varepsilon)$ is the combined relaxation time. Using Matthiessen's rule for scattering events, which are independent from each other, $\tau(\varepsilon)$ can be expressed as[19–22]

$$\tau^{-1} = \tau_b^{-1} + \tau_1^{-1} + \tau_2^{-1} + \tau_3^{-1} \quad , \tag{23}$$

where τ_b is the electronic momentum relaxation time in the bulk matrix, and τ_i ($i = 1, 2, 3$) is that due to scattering at pore/medium interfaces. To find the relaxation time, let us estimate electron mean free path (MFP). When a charge carrier travels a distance L, the average number of its collisions with pores of given size scale is equal to

$$\gamma_i = L A_i c_i \quad , \tag{24}$$

where

$$A_i = \pi\overline{d_i^2} \Big/ 4 = \pi\overline{d_i}^2(1+\alpha_i)/4\alpha_i \quad , \tag{25}$$

is the average classical cross-sectional area. Therefore,

$$\Lambda_i = L/\gamma_i = (A_i c_i)^{-1} \quad , \tag{26}$$

and then τ_i can be found as

$$\tau_i = \frac{\Lambda_i}{v} = \frac{(\alpha_i+2)\overline{d_i}(2m^*)^{1/2}}{3\alpha_i\varphi_i}\varepsilon^{-1/2} \quad , \tag{27}$$

where $v = v(\varepsilon)$ is the electronic velocity. Thus, from Eq. (23) for the combined relaxation time, we obtain

$$\tau(\varepsilon) = \frac{\tau_b}{1 + 3g\tau_b(\varepsilon/2m^*)^{1/2}} \quad , \tag{28}$$

https://doi.org/10.1557/jmr.2015.151 Published online by Cambridge University Press

where g is given in Eq. (12). For definiteness, we will further consider the case of relatively low impurity concentrations, so that the main contribution in the carrier relaxation time at zero porosity is from the scattering on deformation potential of acoustic phonons. Then, setting[19,20]

$$\tau_b = a\varepsilon^{-1/2} \quad , \tag{29}$$

where

$$a = \frac{2\pi\hbar^4\rho u^2}{k_B T(2m^*)^{3/2}D^2} \quad , \tag{30}$$

is the constant for acoustic phonons, ρ is the mass density, u is the longitudinal velocity of the sound, and D is the deformation potential constant, Eq. (28) can be transformed to the form

$$\tau(\varepsilon) = \frac{a\varepsilon^{-1/2}}{1 + 3ag(2m^*)^{-1/2}} \quad . \tag{31}$$

Substituting Eq. (31) into Eqs. (19)–(21), we obtain the following expressions:

$$S = \frac{k_B}{q}\left[\frac{2F_1(\zeta^*)}{F_0(\zeta^*)} - \zeta^*\right] \quad , \tag{32}$$

$$\sigma = \frac{nq^2}{m^*}\frac{bF_0(\zeta^*)}{F_{1/2}(\zeta^*)} \quad , \tag{33}$$

$$b \equiv \frac{2a}{3\sqrt{k_B T}\left[1 + 3ag(2m^*)^{-1/2}\right]} \quad , \tag{34}$$

and

$$P = \frac{nbk_B^2[2F_1(\zeta^*) - \zeta^* F_0(\zeta^*)]^2}{m^* F_0(\zeta^*)F_{1/2}(\zeta^*)} \quad , \tag{35}$$

where $F_n(\zeta^*)$ is given in Eq. (14). Eqs. (32)–(35) for the transport coefficients are valid for an arbitrary level of the Fermi energy.

V. ENHANCEMENT OF THE THERMOPOWER AND POWER FACTOR IN NONDEGENERATE AND DEGENERATELY DOPED POROUS COMPOSITES WITH ALL-SCALE HIERARCHICAL DISORDER

In this section, we will examine peculiarities of the power factor in two limiting cases.

A. Nondegenerate limit

Let us begin from the case of nondegenerate bulk materials with zero porosity. For such a material from Eqs. (32)–(35), one can find well-known classical results[19–24]

$$S_0 = \frac{k_B}{q}\left(2 - \zeta_0^*\right) \quad , \tag{36}$$

$$\sigma_0 = \frac{n_0 q^2\langle\tau_b\rangle}{m^*} \quad , \tag{37}$$

$$P_0 = \frac{n_0 k_b^2\left(2 - \zeta_0^*\right)^2\langle\tau_b\rangle}{m^*} \quad , \tag{38}$$

where ζ_0^* is given by Eq. (15b) and

$$\langle\tau_b\rangle = \frac{4a}{3\sqrt{\pi k_B T}} \quad . \tag{39}$$

For porous materials under consideration, Eqs. (32)–(35) with the use of Eqs. (13) and (15a) are transformed to the form

$$S = S_0\left[1 + \frac{|\ln(1-\phi)|}{2 - \zeta_0^*}\right] \quad , \tag{40}$$

$$\sigma = \frac{\sigma_0(1-\phi)}{1 + 3ag(2m^*)^{-1/2}} \quad , \tag{41}$$

$$P = \frac{P_0(1-\phi)}{1 + 3ag(2m^*)^{-1/2}}\left[1 + \frac{|\ln(1-\phi)|}{2 + \ln(N_c/n_0)}\right]^2 \quad , \tag{42}$$

where ϕ and g are given by Eqs. (11a) and (12).

For relative growth of S and relative change in power factor in this nondegenerate approximation, we obtain

$$\gamma_{s1} \equiv \frac{S - S_0}{S_0} = \frac{|\ln(1-\phi)|}{2 - \zeta_0^*} \quad , \tag{43}$$

and

$$\gamma_{p1} \equiv \frac{P - P_0}{P_0} = \frac{(1-\phi)(\gamma_{s1} + 1)^2}{1 + 3ag(2m^*)^{-1/2}} - 1 \quad , \tag{44}$$

respectively. Before that to examine physical consequences of these equations, let us consider opposite limiting case too.

B. Strongly degenerate limit

For degenerately doped materials from Eqs. (32)–(35), we obtain

https://doi.org/10.1557/jmr.2015.151 Published online by Cambridge University Press

$$S = S_0(1-\phi)^{-2/3} \quad , \tag{45}$$

$$\sigma = \frac{\sigma_0(1-\phi)^{2/3}}{1+3ag(2m^*)^{-1/2}} \quad , \tag{46}$$

$$P = \frac{P_0(1-\phi)^{-2/3}}{1+3ag(2m^*)^{-1/2}} \quad , \tag{47}$$

where S_0, σ_0, and P_0 are the corresponding quantities for strongly degenerate bulk material of zero porosity:

$$S_0 = \frac{\pi^2 k_B^2 T}{3q\varepsilon_F^0} \quad , \tag{48}$$

$$\sigma_0 = \frac{n_0 q^2 a}{m^*\sqrt{\varepsilon_F^0}} \quad , \tag{49}$$

$$P_0 = \frac{2\pi^2(2m^*)^{1/2}ak_B^4T^2}{27\hbar^3\varepsilon_F^0} \quad . \tag{50}$$

Relative growth in S and relative change in power factor in this case are given by

$$\gamma_{s2} = (1-\phi)^{-2/3} - 1 \quad , \tag{51}$$

and

$$\gamma_{p2} = \frac{\gamma_{s2} - 3ag(2m^*)^{-1/2}}{1+3ag(2m^*)^{-1/2}} \quad . \tag{52}$$

According to both Eqs. (40) and (45), the presence of hollow pores of different size scales leads to the enhancement in the thermopower with respect to its value in the bulk material with zero porosity. The enhancement in the absolute value of the Seebeck coefficient and the reduction in electrical conductivity depend on the net effective porosity ϕ. Despite the quite different form of expressions in the right sides of Eqs. (43) and (51), the relative growth of S in both these cases increases monotonically with increasing of the porosity and also (at the given value of the ratio N_s/N_D) with decreasing of characteristic pore sizes $\overline{d_i}$ [see Eq. (12) for φ_{tr}]. Except that, γ_s depends also on the shape parameters of the gamma distribution and increases slightly with increasing of all three parameters α_i.

It is evident that because of the reduction in conductivity, the enhancement in S is not sufficient for the enhancement of the power factor. Indeed, from Eqs. (44) and (52), we conclude that an enhancement in power factor is only possible if the relative growth in S exceeds a definite critical value:

$$\gamma_{s1} > \sqrt{\frac{1+3ag(2m^*)^{-1/2}}{1-\phi}} - 1 \quad , \tag{53}$$

in nondegenerate limit and

$$\gamma_{s2} > 3ag(2m^*)^{-1/2} \quad , \tag{54}$$

in degenerate limit. In the case when the porosity is governed by one length-scale, the conditions (53) and (54) can be rewritten in the form

$$|\ln(1-\phi)| > (2-\zeta_0^*)\left[\sqrt{(1+\Gamma\phi)/(1-\phi)} - 1\right] \quad , \tag{53a}$$

$$\phi > 1 - (1+\Gamma\phi)^{-3/2} \quad , \tag{54a}$$

where

$$\Gamma = 3ag_0(2m^*)^{-1/2}(1+6g_0N_s/N_D)^{-1} \quad , \tag{54b}$$

a is a nondimensional positive parameter and

$$g_0 = \alpha/(\alpha+2)\bar{d} \quad . \tag{54c}$$

We have to recollect that the modulus of the reduced chemical potential in n-type nondegenerate semiconductors satisfies condition $\exp|\zeta_0^*| \gg 1$. Taking these fact into account and carrying out a careful numerical examination, it is not difficult to be convinced that in nondegenerate porous semiconductors, both conditions (53) and (53a) are practically unrealizable, i.e., the increase of the Seebeck coefficient does not compensate the decrease in electrical conductivity. As to the case of a material with strongly degenerated electronic gas, the fulfillment of condition (54a) depends on the value of parameter Γ. At a given value of the effective porosity ϕ, the enhancement of the power factor occurs only if

$$\Gamma < \phi^{-1}\left[(1-\phi)^{-2/3} - 1\right] \quad . \tag{54d}$$

In Fig. 2 are presented the graphs of the function $f(\phi) = 1-(1+\Gamma\phi)^{-3/2}$ in the right-hand side of Eq. (54a) for four different values of Γ. A numerical analysis shows that at $\Gamma \le 0.666$ the condition (54a) is satisfied for all possible values of ϕ. At $\Gamma = 0.67$, 0.7, and 0.8, such a situation occurs only if $\phi > 0.006$, 0.054, and 0.167, respectively. Thus, at $\Gamma > 2/3$, there is a minimum value

$$\phi_{min} = \frac{4}{5\Gamma}\left(1-\frac{2}{3\Gamma}\right) \quad , \tag{54e}$$

so as the enhancement of the power factor occurs only if the porosity $\phi > \phi_{min}$.

https://doi.org/10.1557/jmr.2015.151 Published online by Cambridge University Press

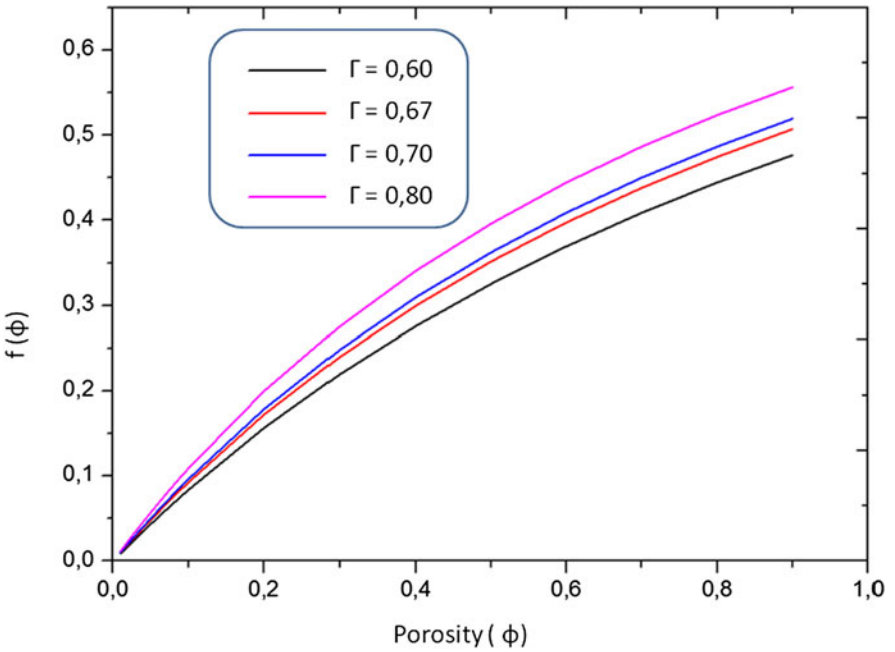


FIG. 2. Graphs of the function $f(\phi) = 1 - (1 + \Gamma\phi)^{-3/2}$ for four different values of Γ.

Note that at small enough porosity values for which $\Gamma\phi \ll 1$, Eq. (54a) gives $\Gamma < 2/3$. This inequality means that in the case when the ratio $N_s/N_D \geq 3a/4(2m^*)^{1/2}$, the enhancement of the power factor becomes possible at an arbitrary value of $\overline{d}$. In the opposite case when

$$N_s/N_D < 3a/4(2m^*)^{1/2} \quad , \qquad (54f)$$

the enhancement of the power factor in degenerate semiconductors with small porosity occurs only if the average pore diameter satisfies the condition $\overline{d} > d_{min}$ where

$$d_{min} = \frac{6\alpha}{(\alpha+2)}\left(\frac{3a}{4(2m^*)^{1/2}} - \frac{N_s}{N_D}\right) \quad . \qquad (54g)$$

Let us take, e.g., $N_s = 10^9\ cm^{-2}$, $N_D = 2.5 \times 10^{16}\ cm^{-3}$, and $m^* = 0.26m_0 = 2.366 \times 10^{-31}$ kg (Si). For the constant a of acoustic phonons [see Eq. (30)] in Si at $T = 200$ K, one can find $a = 1.16 \times 10^{-22}\ kg^{1/2}$ m. Then, Eq. (54g) at "shape" parameter of the distribution, $\alpha = 5$ gives $\overline{d} > 0.54\mu m$. Setting $\overline{d} = 0.6\mu m$, we obtain $g_0 = 1.19 \times 10^6 m^{-1}$ and $\Gamma = 0.6$, i.e., in this case, the enhancement of the power factor can occur at any porosity in the range $\phi \leq 15\%$.

VI. EFFECTIVE THERMOPOWER OF A MULTILAYER COMPOSITE WITH PORES OF VARIOUS SIZE SCALES IN DIFFERENT LAYERS

In the previous section, we have assumed that the pores of different size scales are distributed in the same layer of the thermoelectric material. It is extremely interesting to compare the enhancement of the Seebeck coefficient in such a material with that in multilayer composite consisting of alternating layers with various porosities and pores of different size scales when the pores in each layer have the same size scale. As before, the pores are assumed to be randomly distributed in the layers and described by probability density functions $f(\rho_i)$ given by Eq. (1). For definiteness, we will consider again 3-layer composite: let one of the layers contains small ($d < 100$ nm) nanoscale pores with volume fraction φ_1, the second one pores with intermediate size scale and volume fraction φ_2, and the third layer contains microscale size pores with volume fraction φ_3. The layers are assumed to be perpendicular to the direction of the temperature gradient and having the same volume and thickness. The latter is assumed significantly larger than the maximum value of electron MFP in the layers $\Lambda_{e,i}$. For example, in the case of classical electronic gas, one can find

$$\Lambda_{e,i} = \frac{\langle\tau_b\rangle\sqrt{3k_BT/m^*}}{1 + 3a\alpha_i\varphi_i/(\alpha_i+2)\overline{d_i}(2m^*)^{1/2}} \quad , \qquad (55a)$$

where a and $\langle\tau_b\rangle$ are given by Eqs. (30) and (39), respectively. Since in main thermoelectric materials $\Lambda_e \sim$ 10–100 nm at room temperatures,[25] it is evident that the layers with thickness ~1 mm can be very suitable for experiments.

The electrical conductivity of the composite is given by

https://doi.org/10.1557/jmr.2015.151 Published online by Cambridge University Press

$$\sigma_c = \sigma_0 \left(\sum_i \left[\frac{1 + 3a\alpha_i/(\alpha_i + 2)(2m^*)^{1/2}\overline{d_i}}{3(1-\phi_i)^{\nu}} \right] \right)^{-1} \quad , \tag{55b}$$

where $\nu = 1$ in nondegenerate case and $\nu = 2/3$ in strongly degenerate limit.

Using the fact[26,27] that the thermopower is equivalent to entropy per carrier per charge, and the entropy of a system in local equilibrium conditions is an additive quantity, in Ref. 17, it has been shown that the effective Seebeck coefficient of a multilayer composite can be expressed as

$$S_c = \sum_i n_i S_i / \sum_i n_i \quad , \quad i = 1, 2, 3 \quad , \tag{56}$$

where n_i is the density of free charge carriers in the ith layer, and S_i is the thermopower of the corresponding single layer. Note that there is no discrepancy between different arrangements of the layers with distinct pore size scales. Assuming that the bulk density of electrons n_0 and the ratio N_s/N_D are constants, from Eq. (56) in nondegenerate case, we obtain

$$S_c = S_0 \left[1 + \frac{\sum_i [(1-\phi_i)|\ln(1-\phi_i)|]}{(2-\zeta_0^*)\sum_i (1-\phi_i)} \right] \quad , \tag{57}$$

and relative growth

$$\gamma_{s3} = \frac{\sum_i [(1-\phi_i)|\ln(1-\phi_i)|]}{(2-\zeta_0^*)\sum_i (1-\phi_i)} \quad , \tag{58}$$

where

$$\phi_i = \varphi_i \left[1 + \frac{6N_s\alpha_i}{N_D(\alpha_i+2)\overline{d_i}} \right] \quad . \tag{59}$$

In strongly degenerate case, Eqs. (57) and (58) should be replaced by

$$S_c = S_0 \frac{\sum_i (1-\phi_i)^{1/3}}{\sum_i (1-\phi_i)} \quad , \tag{60}$$

$$\gamma_{s4} = \frac{\sum_i (1-\phi_i)^{1/3}}{\sum_i (1-\phi_i)} - 1 \quad . \tag{61}$$

Using Eqs. (57) or (60) for the thermopower in common with Eq. (55b) for the electrical conductivity, it is not difficult to make analogical calculations for the power factor and its relative change. Furthermore, we will restrict ourselves to the consideration of the thermopower only.

Note that total porosity for ν-layer composite material containing layers of various volume V_i and porosity φ_i is given by average porosity

$$\varphi = \sum_{i=1}^{\nu} \varphi_i V_i \Big/ \sum_{i=1}^{\nu} V_i \quad , \tag{62a}$$

where $\varphi_i V_i$ is the total volume of the pores in a layer with number i. If the layers have the same volume ($V_i = V_0$), Eq. (62a) gives $\varphi = \left(\sum_{i=1}^{\nu} \varphi_i \right) / \nu$ or for 3-layer composite

$$\varphi = (\varphi_1 + \varphi_2 + \varphi_3)/3 \quad . \tag{62b}$$

A simple comparison of Eq. (58) with Eq. (43) and Eq. (61) with Eq. (51) shows that the enhancement in the absolute value of S in the multilayer composite is considerably less than that in single layer composite with multiscale size pores:

$$\frac{\gamma_{s3}}{\gamma_{s1}} = \frac{\sum_i [(1-\phi_i)|\ln(1-\phi_i)|]}{|\ln(1-\phi)|\sum_i (1-\phi_i)} \quad , \tag{63}$$

in nondegenerate case and

$$\frac{\gamma_{s4}}{\gamma_{s2}} = \frac{\left[\sum_i (1-\phi_i)\right]^{-1} \sum_i (1-\phi_i)^{1/3} - 1}{(1-\phi)^{-2/3} - 1} \quad , \tag{64}$$

in the case of strongly degenerate electronic gas. In Eqs. (63) and (64), ϕ_i and ϕ can be expressed by the same relations, which are given in Eqs. (10) and (11a), respectively. It is evident that to compare the enhancement in the thermopower of the 3-layer material and homogeneous material with the same volume fraction of the pores in each one, for the total porosity φ in Eq. (11a) must be used by the value given by Eq. (62b) so that the materials differ only in physical arrangement of the pores.

Setting, for example, $\overline{d_1} = 10$ nm, $\overline{d_2} = 0.2$ μm, $\overline{d_3} = 1$ μm, $\alpha_1 = 8$, $\alpha_2 = 6$, $\alpha_3 = 3$, and $\varphi_1 = \varphi_2 = \varphi_3 = 0.05$, from Eq. (63) at $N_s = 10^9$ cm^{-2} and $N_D = 10^{16}$ cm^{-3}, we obtain $\gamma_{s3}/\gamma_{s1} = 0.767$. However, for heavily doped samples at $N_D = 2.5 \times 10^{16}$ cm^{-3} and the same values of the other parameters, Eq. (64) gives $\gamma_{s4}/\gamma_{s2} = 0.886$.

Thus, in both these limiting cases, the medium with multiscale size pores in the same host material provides

https://doi.org/10.1557/jmr.2015.151 Published online by Cambridge University Press

stronger enhancement in the thermopower compared with that in layered composite in which each layer contains pores of single length-scale: more than 30% stronger enhancement in the case of nondegenerate electronic gas and ~10% in strongly degenerate case.

It is not difficult to see that the enhancement in the material with multilength-scale pores exceeds that also in the case of an identical material with single-scale pores when they have the same total porosity. Really, the relative growth of the thermopower in a material with nondegenerate electronic gas and single-scale pores is given by

$$\gamma_s = \frac{|\ln(1-\phi_s)|}{2-\zeta_0^*} \quad , \tag{65a}$$

where

$$\phi_s = \varphi\left[1+\frac{6N_s\alpha}{N_D(\alpha+2)\overline{d}}\right] \quad . \tag{65b}$$

A comparison of Eqs. (65a) and (43) shows immediately that the ratio γ_s/γ_{s1} is always less than 1. For example, consider a material with monoscale pores described by $\overline{d} = 0.2$ μm, $\alpha = 6$, and $\varphi = 0.05$. Then for the same values $N_s = 10^9$ cm^{-2} and $N_D = 10^{16}$ cm^{-3}, one can find $\phi_s = 0.051$ and $\gamma_s/\gamma_{s1} = 0.669$. In the case of microscale pores with $\overline{d} = 1$ μm, $\alpha = 3$, and the same porosity $\varphi = 0.05$, the ratio is $\gamma_s/\gamma_{s1} = 0.655$. Thus, the medium with multiscale size pores provides ~1.5 times stronger enhancement in the thermopower than a material with monoscale porosity.

It is evident that by combining the significant reduction of lattice thermal conductivity predicted in Refs. 15 and 16 and possible enhancement in the power factor due to the increasing value of the thermopower, high thermoelectric performance of porous materials can be achieved.

VII. CONCLUSIONS

The main results of this paper can be summarized as follows:

(1) The presence of hollow pores of different size scales randomly distributed throughout the matrix thermoelectric material leads to the enhancement of the thermopower and the reduction of the electrical conductivity relative to their values in the bulk material with zero porosity.

(2) A theoretical model based on the gamma distribution of the pore sizes is proposed to calculate the changes in transport coefficients. The results show that high density of nano- and microscale pores could cause effective trapping of charge carriers, which leads to additional enhancement in the Seebeck coefficient and reduction in the electrical conductivity. Obviously, the influence of trapping on transport coefficients is especially sensible in nondegenerate semiconductors.

(3) Analytical expressions are found for the thermopower, electrical conductivity, and power factor for the porous material at the arbitrary level of the Fermi energy in the case when the main contribution in the carrier relaxation time at zero porosity is from the scattering on deformation potential of acoustic phonons.

(4) It is shown that the semiconductor with nondegenerate electronic gas and pores of different size scales in the same host material has an advantage with respect to a multilayer composite of different layers of which contain only pores of the same length-scale, since it provides stronger enhancement in the Seebeck coefficient.

(5) Simple expressions for relative growth of the Seebeck coefficient (γ_s) and change of the power factor (γ_p) are obtained for porous thermoelectric materials with nondegenerate and strongly degenerate electronic gas.

(6) Necessary conditions for γ_s are found at which thermoelectric power factor increases in spite of the reduction in electrical conductivity. It is shown that in nondegenerate porous semiconductors, the increase of the Seebeck coefficient does not compensate the decrease in electrical conductivity. Unlike this, in materials with strongly degenerate electronic gas, the enhancement in power factor occurs for all possible values of porosity ϕ, if nondimensional parameter Γ [given by Eq. (54b)] is less than 2/3.

(7) The relative growth of S increases monotonically with increasing of the volume fraction of the pores and decreasing of the average pore size. Except that, γ_s depends slightly on the shape parameters of the gamma distribution and increases with increasing of numerical values of these parameters.

ACKNOWLEDGMENT

The authors would like to acknowledge the financial support of the Project 2012 KRIPIS funded by the ESPA program 2007–2014.

REFERENCES

1. S.V. Faleev and F. Leonard: Theory of enhancement of thermoelectric properties of materials with nanoinclusions. *Phys. Rev. B* **77**, 214304 (2008).
2. J.H. Lee, G.A. Galli, and J.C. Grossman: Nanoporous Si as an efficient thermoelectric material. *Nano Lett.* **8**, 3750 (2008).
3. J.G. Snyder and E.S. Toberer: Complex thermoelectric materials. *Nat. Mater.* **7**, 105–114 (2008).
4. H. Lee, D. Vashaee, D.Z. Wang, M.S. Dresselhaus, Z.F. Ren, and G. Chen: Effects of nanoscale porosity on thermoelectric properties of SiGe. *J. Appl. Phys.* **107**, 094308 (2010).
5. J.F. Li, W.S. Liu, L.D. Zhao, and M. Zhou: High-performance nanostructured thermoelectric materials. *Nat. Asia Mater.* **2**, 152–158 (2010).

https://doi.org/10.1557/jmr.2015.151 Published online by Cambridge University Press

6. C. Vineis, A. Shakouri, A. Majumdar, and M. Kanatzidis: Nanostructured thermoelectrics: Big efficiency gains from small features. *Adv. Mater.* **22**, 3970 (2010).
7. T.C. Harman, P.J. Taylor, M.P. Walsh, and B.E. LaForge: Quantum dot superlattice thermoelectric materials and devices. *Science* **297**, 2229 (2002).
8. K. Biswas, J. He, Q. Zhang, C. Uher, V. Dravid, and M.G. Kanatzidis: Strained endotaxial nanostructures with high thermoelectric figure of merit. *Nat. Chem.* **3**, 160 (2011).
9. K. Biswas, J. He, I.D. Blum, C.I. Wu, T.P. Hogan, D.N. Seidman, V.P. Dravid, and M.G. Kanatzidis: High-performance bulk thermoelectrics with all-scale hierarchical architectures. *Nature* **489**, 414 (2012).
10. J. He, M.G. Kanatzidis, and V.P. Dravid: High performance bulk thermoelectric via a panoscopic approach. *Mater. Today* **16**, 166–176 (2013).
11. L.G. Fel, Y.M. Strelniker, and D.J. Bergman: Enhancement of power factor in a thermoelectric composite with a periodic microstructure. *Proceedings MRS Spring Meeting, San Francisco*, Vol. **626**, Z6.5, April 2000.
12. J. Martin, L. Wang, L. Chen, and G.S. Nolas: Enhanced Seebeck coefficient through energy-barrier scattering in PbTe nanocomposites. *Phys. Rev. B* **79**, 115311 (2009).
13. H.H. Huang, M.P. Lu, C.H. Chiu, L.C. Su, C.N. Liao, J.Y. Huang, and H.L. Hsieh: Enhanced Seebeck coefficient of bismuth telluride compounds with graded doping. *Appl. Phys. Lett.* **103**, 163903 (2013).
14. N. Neophytou, X. Zianni, H. Kosina, S. Frabboni, B. Lorenzi, and D. Narducci: Simultaneous increase in electrical conductivity and Seebeck coefficient in highly boron-doped nanocrystalline Si. *Nanotechnology* **24**, 205402 (2013).
15. R.H. Tarkhanyan and D.G. Niarchos: Effect of pore sizes on the reduction in lattice thermal conductivity of nano to micro scale porous materials. *J. Electronic Mater.* **43**, 3808–3811 (2014).
16. R.H. Tarkhanyan, A. Ioannidou, and D.G. Niarchos: Lattice thermal conductivity in nano to micro scale porous materials. *Metall. Mater. Trans. E* **1**, 145–152 (2014).
17. R.H. Tarkhanyan and D.G. Niarchos: Seebeck coefficient of graded porous composites. *J. Mater. Res.* **28**, 2316 (2013).
18. M.V. Jambunathan: Some properties of beta and gamma distributions. *Ann. Math. Stat.* **25**, 401–405 (1954).
19. J.M. Ziman: *Electrons and Phonons* (Oxford University Press, Oxford, 1960).
20. A.I. Ansel'm: *Introduction to Semiconductor Theory* (Mir, Moscow; Prentice-Hall, Englewood Cilffs, New Jersey, 1981).
21. C. Kittel: *Introduction to Solid State Physics* (Wiley, New York, 1971).
22. M. Lundstrom: *Fundamentals of Carrier Transport*, 2nd ed. (Cambridge University Press, Cambridge, 2000).
23. G. Chen: *Nanoscale Energy Transport and Conversion* (Oxford University Press, NewYork, 2005).
24. P.Y. Yu and M. Cardona: *Fundamentals of Semiconductors*, 3rd ed. (Springer, Berlin, 2003).
25. G. Chen, M.S. Dresselhaus, G. Dresselhaus, J.P. Fleurial, and T. Caillat: Recent developments in thermoelectric materials. *Int. Mater. Rev.* **48**, 45–66 (2003).
26. H.B. Callen: *Thermodynamics* (Wiley & Sons, New York, 1960).
27. S.R. de Groot and P. Mazur: *Non-Equilibrium Thermodynamics* (North-Holland Com., Amsterdam, 1962).

https://doi.org/10.1557/jmr.2015.151 Published online by Cambridge University Press